ELSEVIER

Physics of the Earth and Planetary Interiors 106 (1998) 139–153

PHYSICS OF THE EARTH AND PLANETARY INTERIORS

Energetic balance in scaling organization of fracture tectonics

Claude J. Allègre [b,c], Pierre Shebalin [a], Jean-Louis Le Mouël [b,*], Clément Narteau [b]

[a] *International Institute of Earthquake Prediction Theory and Mathematical Geophysics, Warshavskoye shosse, 79, korp. 2, 113156 Moscow, Russian Federation*

[b] *Institut de Physique du Globe de Paris, 4, Place Jussieu, 75252 Paris Cedex 05, France*

[c] *Université Paris VII, 2, Place Jussieu, 75252 Paris Cedex 05, France*

Received 24 February 1997; accepted 2 July 1997

Abstract

This paper presents a development of the seismicity model S.O.F.T. (scaling organization and fracture tectonics). We remain in the frame of this simple model, which is based on an energy splitting combined with a renormalization group approach. Redistribution of energy over the entire considered domain after strong events was introduced in the previous model. The present version displays some general features of real seismicity, such as Gutenberg–Richter law, Omori law of temporal decrease of the aftershock activity, seismic cycle ('quiet' periods with a background seismic activity, periods of foreshock and aftershock activity). This is shown by numerical experiments in both the single domain case and in the case of exchange of energy between several domains. © 1998 Elsevier Science B.V.

1. Introduction

We consider a hierarchy of scales in a fault zone (King, 1983). The earthquake is a critical phenomenon which takes place when fracturing becomes coherently self-organized at different scales (Allègre et al., 1982, 1995; Ito and Matsuzaki, 1990; Keilis-Borok, 1990). The fault zone is modeled by a domain which permanently receives some energy from outside. This energy is then dissipated through fracturing at different scales. Probabilities of fracturing at different scales are determined using a kind of renormalization group technique (Wilson, 1979) which we named scaling technique (Allègre et al., 1982; Turcotte, 1992). At the lowest (most detailed) scale, this probability is a function of the density of energy per surface (volume) unit. Each rupture causes a total loss of energy in the corresponding part of the domain (Allègre et al., 1995; Kanamori and Anderson, 1975). Later the 'lost' part of the domain is gradually reloaded due to the redistribution of energy through slow deformation (creep: King, 1978; Kranz, 1979).

In the frame of the present model, the scenario of occurrence of strong earthquakes in a domain is as following. During a quiet period the energy coming from outside increases little by little the probability of fracturing. Only the smallest events occur. At some moment the system starts the coherent fracturing over lowest to medium scales. This is expressed in foreshock activity. When the coherent self-organization achieves the highest scales, a strong earthquake occurs. As a result, a big part of the volume of the domain looses its energy. This diminishes the

* Corresponding author. Tel:. +33-01-44-27-39-04; fax: +33-01-44-27-33-73; e-mail: lemouel@ipgp.jussieu.fr

PII S0031-9201(97)00079-4

size of the remaining sound (effective) volume. As a consequence, the process cannot any more reach the highest level scales, and only less strong earthquakes can occur. Part of the released energy is passed to the remaining effective volume in which the density of energy and the fracturing probability increase. This starts the aftershock activity. Simultaneously the redistribution of energy by means of creep is started. Although this process is slow, it is enough to diminish step by step the density of energy. This forces a gradual slowing-up of the aftershock sequence. Finally, the fall of the density of energy passes some limit, the reloading process starts, and the cycle repeats itself (Blanter et al., 1997).

The balance of energy in such a system can also be so that all the received energy has the time to dissipate at intermediate-level scales, giving raise only to moderate magnitude earthquakes. But a small additional energy can lead to the occurrence of a strong earthquake. To model such a behavior we consider later a multidomain case; in this more complex model additional injections of energy, due to exchanges between the domains, are added to the constant rate of energy which is provided to the considered domain from outside. The intensity of those injections is not permanent in time.

In the previous paper on S.O.F.T. model (Allègre et al., 1995), we started with similar energy considerations. But we concentrated on the analysis of the behavior of the system during a time interval including a strong earthquake, rather than an entire cycle. The weakness was in the aftershock sequences.

In the present paper we introduce a redistribution of energy over the entire domain by a creep mechanism. This allows us to obtain more realistic aftershock sequences, with a temporal decrease of their intensity (Omori law), and also to reproduce the entire seismic cycle. We also study here more carefully the Gutenberg–Richter law at different stages of the seismic process.

2. Model of fault zone

As in Allègre et al. (1995), we model a fault zone by a set of domains which represent neighboring segments of this zone (Fig. 1). This system continuously receives energy from its tectonic environment. Each domain has its own behavior, but in addition, all the domains interact with each other through an exchange of energy in various forms (seismic, elastic, tectonics). We will first develop the theory for one domain, then indicate how to extend the model to the case of interacting domains.

2.1. Theoretical formalism

This formalism resumes the general theoretical basis which was described in the previous paper (Allègre et al., 1995). We shall not describe it in detail, but focus on the changes brought to the model. For the analysis of the state of the chosen domain we consider successive time moments $t, t+1, t+2\ldots$ Our model is deliberately intrinsically discrete, and the time unit is unreducible. Let $E(t)$ be the total energy the domain possesses at the time moment t, $\Delta E(t)$ the amount of energy which the domain receives during the time interval $(t, t+1)$ from outside (from plate tectonics and energy exchange with other domains), and $R(t)$ the energy lost by the domain in earthquakes (fracturing, redistribution of strain, seismic waves and heat generation by non-elastic motions):

$$E(t+1) = E(t) + \Delta E(t) - R(t) \qquad (1)$$

We shall call the component $\Delta E(t)$ the loading component of the energy rate, and $R(t)$ the dissipation component. The analysis of the balance, or competition, between loading and dissipation is a basic feature of this paper.

We consider a two-dimensional model. During the continuous process of loading and dissipation of energy, the different parts of the domain become obviously characterized by different densities of elastic energy. We model such an heterogeneity by the following simple assumption: at moment t all the energy of the domain is homogeneously distributed over only a part $S(t)$ of the total surface S_0 of the domain. Thus we assume that the remaining part, $S_0 - S(t)$, has completely lost its elastic energy. If the density of energy per surface unit $E(t)/S(t)$ exceeds some threshold ε, then this energy excess can result in generating new cracks and developing ancient cracks by growth.

We use the same scaling technique as in Allègre et al. (1982, 1995) and Allègre and Le Mouël (1994).

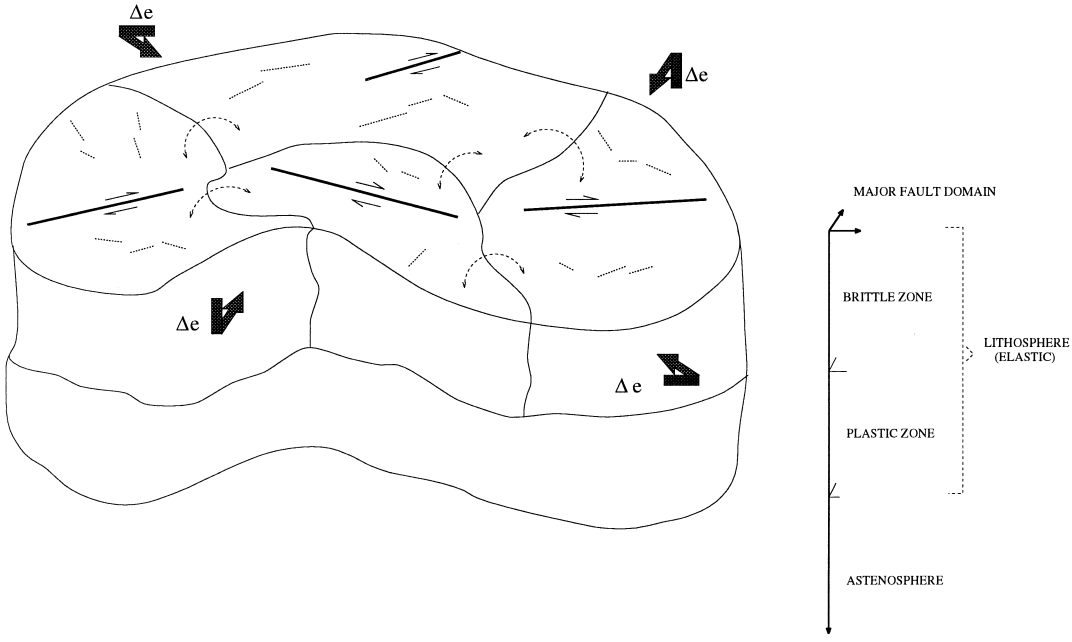

Fig. 1. Illustration of a model of fault zone. Four domain (separated by a solid line) receive an elastic energy (Δe) from the stress applied to their boundary by plates tectonics. The fault zone is supposed to be composed of a brittle layer above a plastic one. Fat lines represent the major faults, dotted lines represent the minor faults, and dashed lines represent the exchange of energy between two domains. Around each segment, we define a three-dimensional domain with specific geometries, extending to a prescribed depth. The three-dimensional domains are those where the fracture occur.

We divide the considered domain into a hierarchy of embedded grids of (3×3) cells. L is the maximum number of levels of this hierarchy. At the lowest scale level (1) we have N elementary cells. The probability $p_1(t)$ of fracturing for each elementary cell depends on the excess of the energy density:

$$p_1(t) = \frac{n_1(t)}{N(t)} = 1 - \exp\left(-\alpha \left(\frac{E(t)}{S(T)} - \varepsilon \right) \right) \quad (2)$$

$n_1(t)$ being the number of elementary cells where a crack is created during the time interval $(t,t+1)$, α a coefficient. This formula is a natural generalization of the linear one we used in the previous paper.

At the next scale (level 2) we consider $N/9$ cells comprising (3×3) elementary cells. At level 3 we have $N/9^2$ cells comprising (3×3) cells of level 2 etc. From the level k to the level $k+1$ the fracturing is transmitted according to the following rule: if at least three cells of level k aligned along the fault zone major axis are cracked, then the corresponding cell of level $k+1$ is also cracked (Fig. 2). We do not introduce any time delay for transmitting fracturation from level k to level $k+1$ (but the whole process of going through all the scales is made during the chosen unit of time). Thus, as in Allègre and Le Mouël (1994), the probability of fracturing at level k during the time interval $(t,t+1)$ is defined recursively as:

$$p_k(t) = P\left[p_{k-1}(t) \right] \quad (3)$$

with:

$$P(x) = 3x^3(1-x)^6 + 18x^4(1-x)^5 + 45x^5(1-x)^4 + 57x^6(1-x)^3 + 36x^7(1-x)^2 + 9x^8(1-x) + x^9$$

We consider the fracturation of one cell at level k during the time interval $(t,t+1)$ as an earthquake occurring at time t (or micro-earthquake for lower levels). The magnitude of this earthquake is naturally proportional to the level k. We shall discuss this in more detail later. The fracturing at the highest level L is the strongest possible earthquake in the consid-

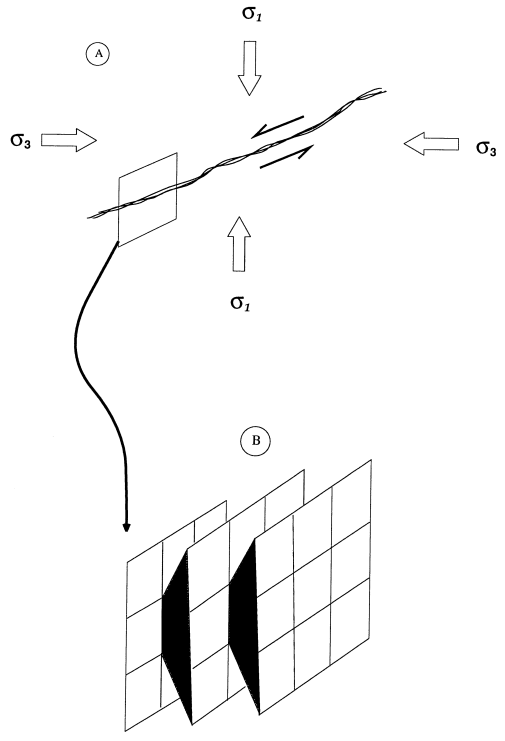

Fig. 2. This cartoon illustrates the scaling technique derived from the renormalization group theory used by Allègre and Le Mouël (1994). The domain (A) is divided into subdomains (B), the subdomains are divided into smaller ones… until the elementary domain scale is reached. We used a grid of 3×3 domains. (Allègre et al., 1995).

ered domain (Aki, 1984); this highest level can be reached only if the current effective surface $S(t)$ of the domain is close to the total surface S_0. In a general way we suppose that only the part $S(t)/S_0$ of all cells can generate quakes; more precisely, the number of earthquakes (micro-earthquakes) of level k which occur during the time interval $(t,t+1)$ is defined as:

$$K_k(t) = \left[p_k(t)\, N_k \frac{S(t)}{S_0} + \delta \right] \tag{4}$$

where $N_k = N/9^{k-1}$ is the total number of cells of level k; [] means integer part; δ is constant ($\delta < 1.0$). Eq. (4) controls the maximum level which the system can reach at time t. This replaces a little bit more artificial approach in the previous paper.

We assume as earlier that the energy r_k released in one earthquake at level k is proportional to the linear size of the corresponding cell at the 3rd power, $r_k = \lambda 3^{3k}$ (λ being a scaling parameter). Combining with Eq. (4), we obtain the dissipation component of the energy:

$$R(t) = \lambda \sum_{k=1}^{L} K_k(t) 3^{3k} \tag{5}$$

As in S.O.F.T. 1, we assume that, after earthquakes have occurred, the corresponding subdomains have completely lost their energy. The part of this energy which has not been lost in elastic waves, or heat, has gone to the remaining part of the domain. This process is assumed to need some time to be completed. The size of the effective surface is reduced by a certain amount $\Delta S_1(t)$:

$$\Delta S_1(t) = \mu \sum_{\tau = t - \sigma_1 + 1}^{t} \frac{R(\tau)}{\sigma_1} \tag{6}$$

where μ is scaling parameter, and σ_1 defines the delay, $\sigma_1 \geq 1$.

As the most significant change of the model in comparison with the previous one, we introduce here a slow redistribution of energy in the entire domain. After Blanter and Shnirman (1996), we suppose the creep being the mechanism of this redistribution.

Energy comes continuously to the domain from outside, and part of it goes to the destroyed subdomains. In addition, through comparatively very slow movements (creep), strains are redistributed so that parts of the destroyed subdomains are reloaded faster than simply due to the external energy injection. This results in the apparent regeneration of the effective surface with the rate $\Delta S_2(t)$. In reality this means only that the distorted subdomains take away some energy from the subdomains in which the concentration of energy is high.

The apparent effective surface regeneration rate $\Delta S_2(t)$ should depend on the relative size of $S(t)$. We take:

$$\Delta S_2(t) = \frac{S_0 - S(t)}{\sigma_2} \tag{7}$$

where we suppose $\sigma_2 \gg \sigma_1$.

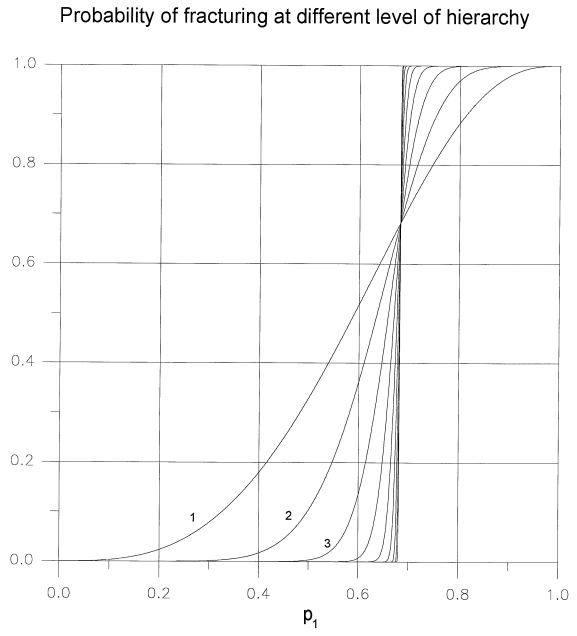

Fig. 3. Probability of fracturing at different levels of the hierarchy. This probability is defined by Eq. (3). All curves intersect at the critical value $p_1 = 0.6823$: $p_{k+1}(x) \geq p_k(x)$, if $x \geq 0.6823$.

Finally the evolution of the effective surface $S(t)$ results from a competition between reduction and increase:

$$S(t+1) = S(t) - \Delta S_1(t) + \Delta S_2(t) \qquad (8)$$

Remark: Redistribution of energy (through the creep) consumes some energy. For simplicity we assume that this energy rate is constant (i.e., that its variations are negligibly small in comparison with both loading and dissipation components in Eq. (1) (which implies that the constant part of the creep energy is subtracted from the loading component ΔE).

Now we can qualitatively describe how the model generates self-organized critical phenomena similar to the tectonic earthquakes. We can summarize its behaviour in the following way.

The domain permanently receives energy from outside. This energy input increases the energy density per surface unit at elementary (level 1) for cells which form the 'effective surface'. This increases the probability of fracturing at this level, and consequently the number of micro-earthquakes of level 1. When the probability $p_1(t)$ is lower than the critical value (see Fig. 3) the probabilities $p_k(t)$ are close to 0 for the upper levels of our scale hierarchy $k = 2, 3, \ldots, L$. When $p_1(t)$ comes close to the critical probability, coherent fracturing reaches upper levels, and foreshock activity starts. Finally $p_1(t)$ passes the critical value, and a strong earthquake (of the highest level L) occurs. A big part of the energy which the system had accumulated before is lost due to the strong earthquake; but the effective surface also falls down, although more slowly due to the time constant σ_1, and the energy density in the remaining part of the domain can increase again, resulting in an increase of $p_1(t)$. This generates the sequence of aftershocks. Their number per time unit is high at the beginning. But, due to the redistribution of the energy through creep, the density of energy per surface unit rapidly falls down, and the aftershock activity decreases. At the end of the cycle the long process of reloading starts and it continues until the new perturbation.

The behavior of the system varies despondently on the values of the parameters. We shall see different examples in the numerical experiments later on.

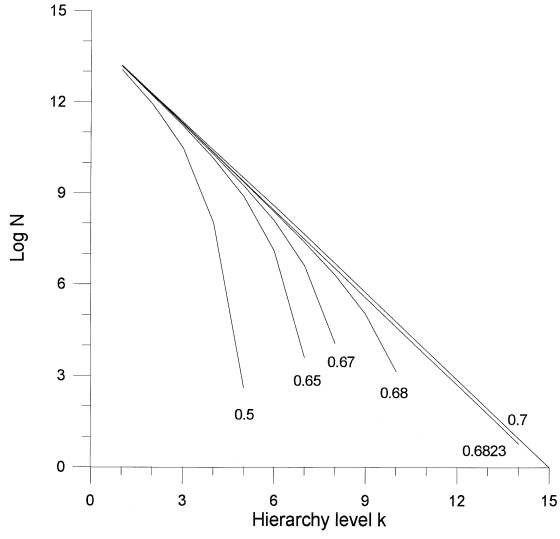

Fig. 4. Theoretical magnitude–frequency graphs for one elementary time interval and different values of p_1. Hierarchy level k is used as earthquake magnitude according to Eq. (13). Graphs are constructed using Eq. (4) with $S(t) = S_0$, $L = 15$, $\delta = 0.1$.

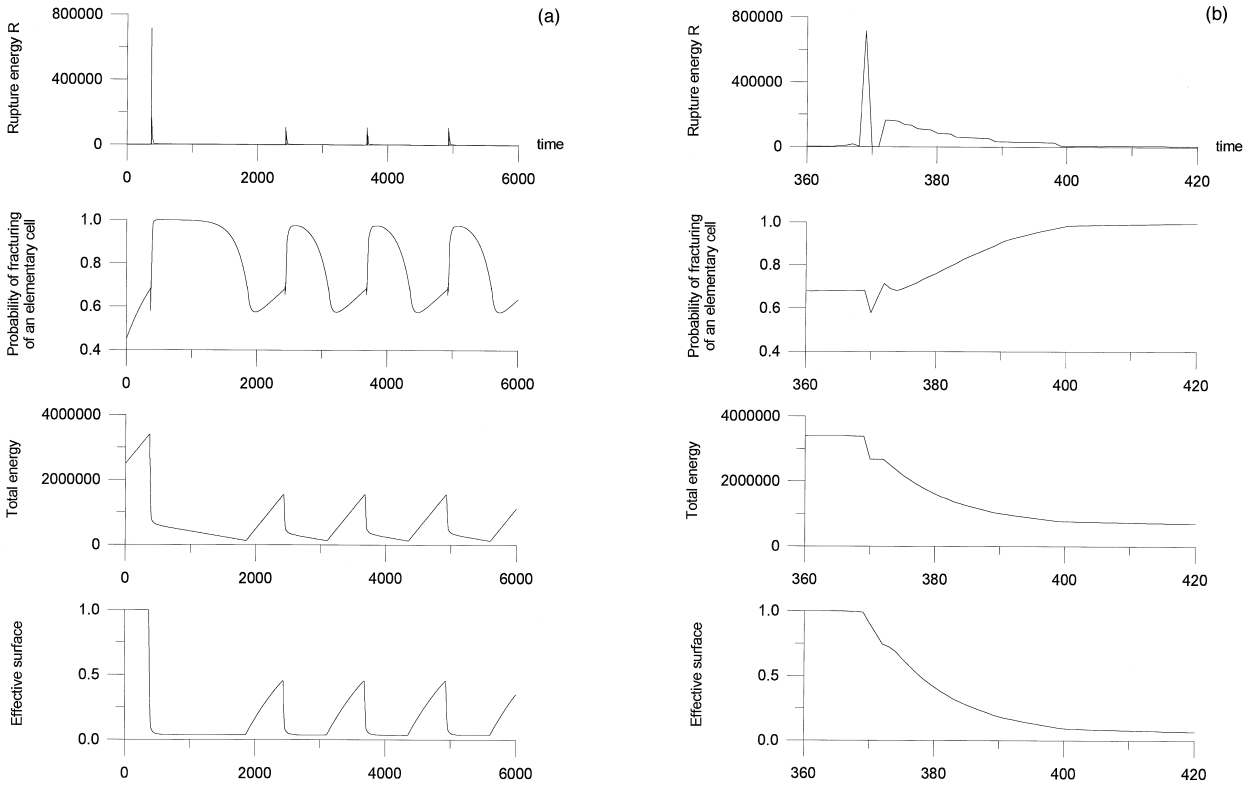

Fig. 5. Typical experiment in the single domain case; (a) on a short time span (b) on a long time span. Time variation of R, p_1, E, and S are shown. In this typical experiment the following parameters of the model are used: $E_0 = 2.5\times10^6$; $\Delta E_0 = 2.5\times10^3$; $\alpha = 6.0\times10^{-7}$; $\varepsilon = 1.5\times10^6$; $\delta = 0.1$; $\lambda N = 0.1$; $\mu = 3.4\times10^{-7}$; $\sigma_1 = 3$; $\sigma_2 = 1000$; $L = 15$.

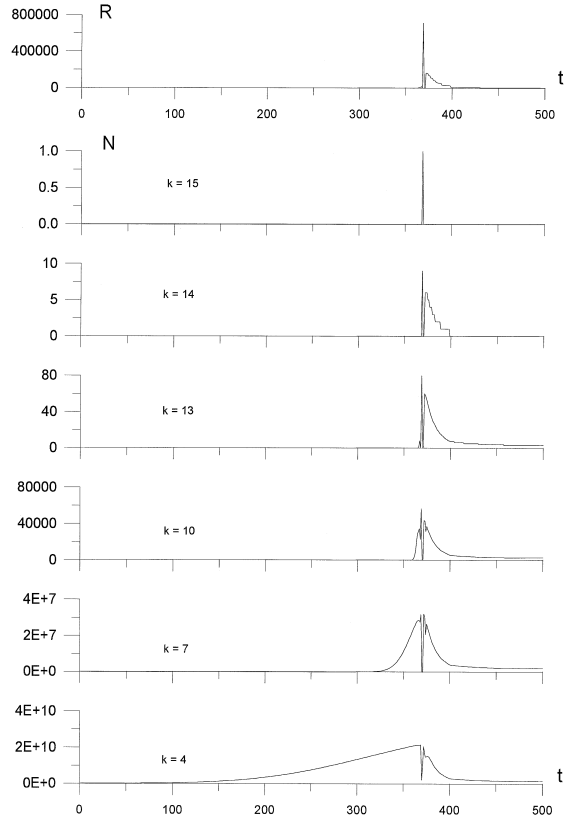

Fig. 6. Time variation of the number of events per unit of time, at different levels of hierarchy, for the typical experiment. Values of the parameters are as for Fig. 5.

We shall consider first the simple case of the single domain with a constant value $\Delta E(t) = \Delta E_0$ of the rate of loading. In the multidomain case we will simplify the approach proposed in Allègre et al. (1995). Only one domain is considered, but $\Delta E(t)$ contains a time varying component formed by the sum of energy supplies coming from its neighboring domains:

$$\Delta E(t) = \Delta E_0 + \sum_i m_i R_i(t) \qquad (9)$$

Index i marks the different domains, $R_i(t)$ is the dissipation energy (Eq. (5)) of domain R_i. In numerical experiments we can iteratively use different realizations of $R_i(t)$ obtained in previous single domain and multidomain cases.

2.2. Gutenberg–Richter law

In real seismicity the distribution of earthquake magnitudes follows the Gutenberg–Richter law (Kanamori and Anderson, 1975):

$$\log(N) = -bM + \text{const}, \qquad (10)$$

where N is the number of earthquakes with magnitude M during some (rather long) time interval and b the slope of the magnitude–frequency graph. The parameter b varies in the range of 0.6–1.4 according to the different seismic zones (Gutenberg and Richter, 1954; Utsu, 1965; Hattori, 1974). The b value can also vary in time; in addition, the magnitude–frequency graph can have a downward bend at large magnitude values, and this bend can also vary in time. Those effects are interesting when analysing the different stages of the seismic process and its predictability (Narkunskaya and Shnirman, 1990).

To construct magnitude–frequency graphs we have first to define the earthquake magnitude in our model. We mentioned above that the magnitude should be a linear function of the level of the hierarchy of scales k. Magnitude is indeed characteristic of

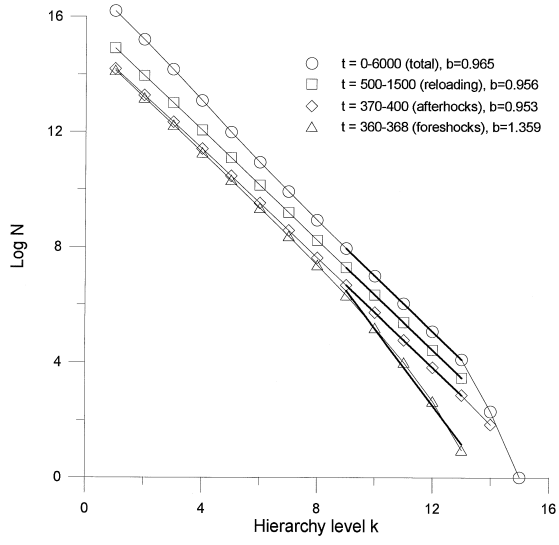

Fig. 7. Magnitude–frequency graphs for different stages of the seismic process. We take the hierarchy level k as the magnitude according to Eq. (13). The typical experiment (Fig. 5) parameters values are used. The b value for all curves is calculated by the least squares method on the interval $9 \le k \le 13$. The slope for foreshocks ($t = 360–368$, see Fig. 5a) is significantly higher than the slope for aftershocks, the reloading period, and the total considered time interval.

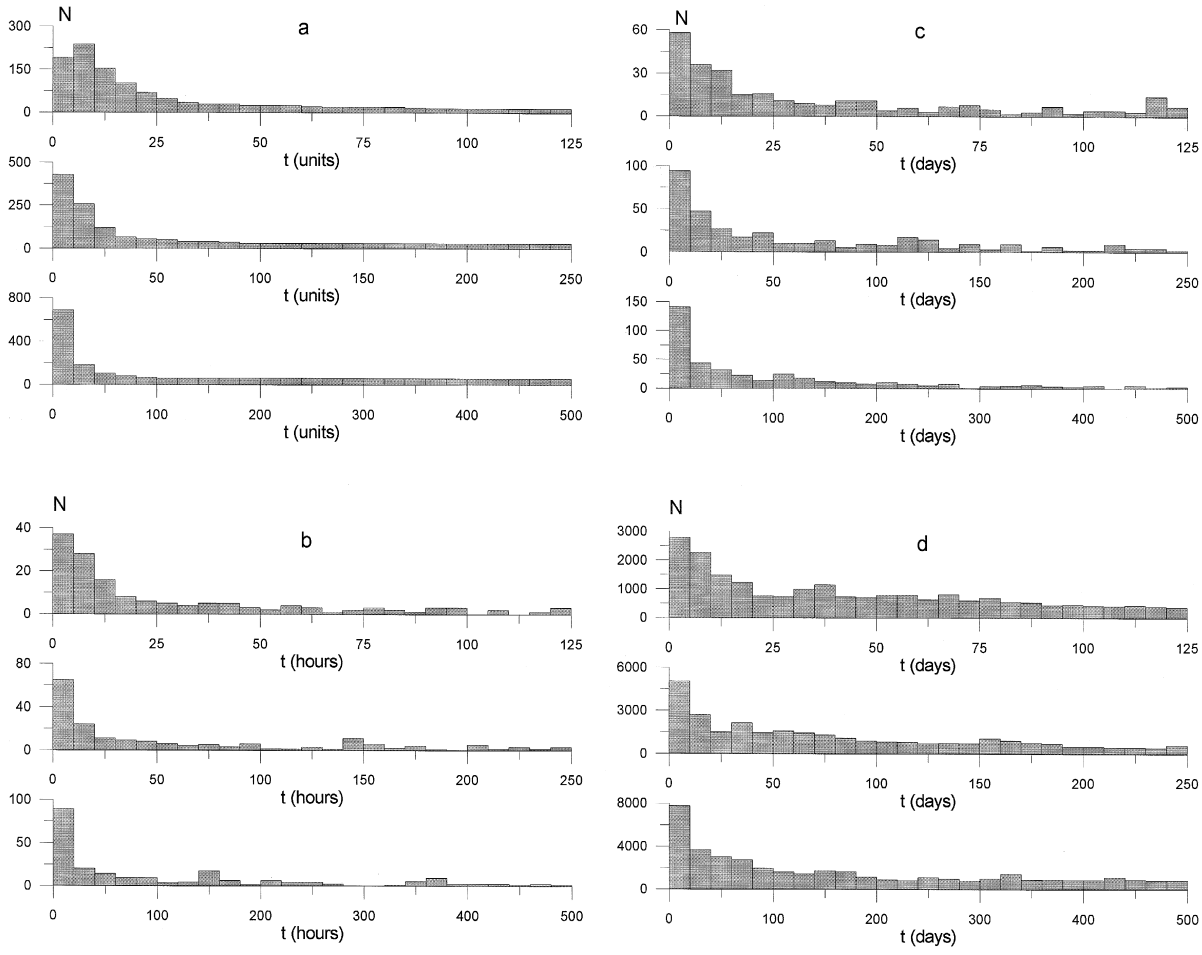

Fig. 8. Self-similarity of aftershock sequences. (a) Typical experiment of the model; (b) aftershocks $M \geq 4$ of the earthquake 26/5/1983 in Japan, $M = 7.7$; (c) aftershocks $M \geq 4$ of the Southern Kurils earthquake 4/10/1994, $M = 8.1$; (d) aftershocks $M \geq 2$ of the Landers earthquake 28/6/1992, $M = 6.7$ in California. We consider histograms of the number of aftershocks in the fixed length boxes as function of time after the main shock. Three different time scales (changing like 1, 2, 4) are shown for each example. The picture for the typical experiment of our model is very similar to those for real aftershock series. Self-similarity of the real aftershock sequences is due to the Omori law.

the size of the earthquake; the relationship between the magnitude and the focal surface S is well known (Utsu, 1961):

$$M = C \log(S) + \text{const} \tag{11}$$

The coefficient C varies from 0.6 to 1.4 according to the different authors (Okal and Romanowicz, 1994); the most commonly used value is $C = 1$.

In our model we can consider the focal surface to be proportional to the size of the cell of each level k of hierarchy. Thus:

$$M = C \log\left(\frac{S_0}{N} 9^{k-1}\right) + \text{const} = C \log(9k) + \text{const} \tag{12}$$

Taking $C = \dfrac{1}{\log(9)} = 1.05$, we have:

$$M = k + \text{const} \tag{13}$$

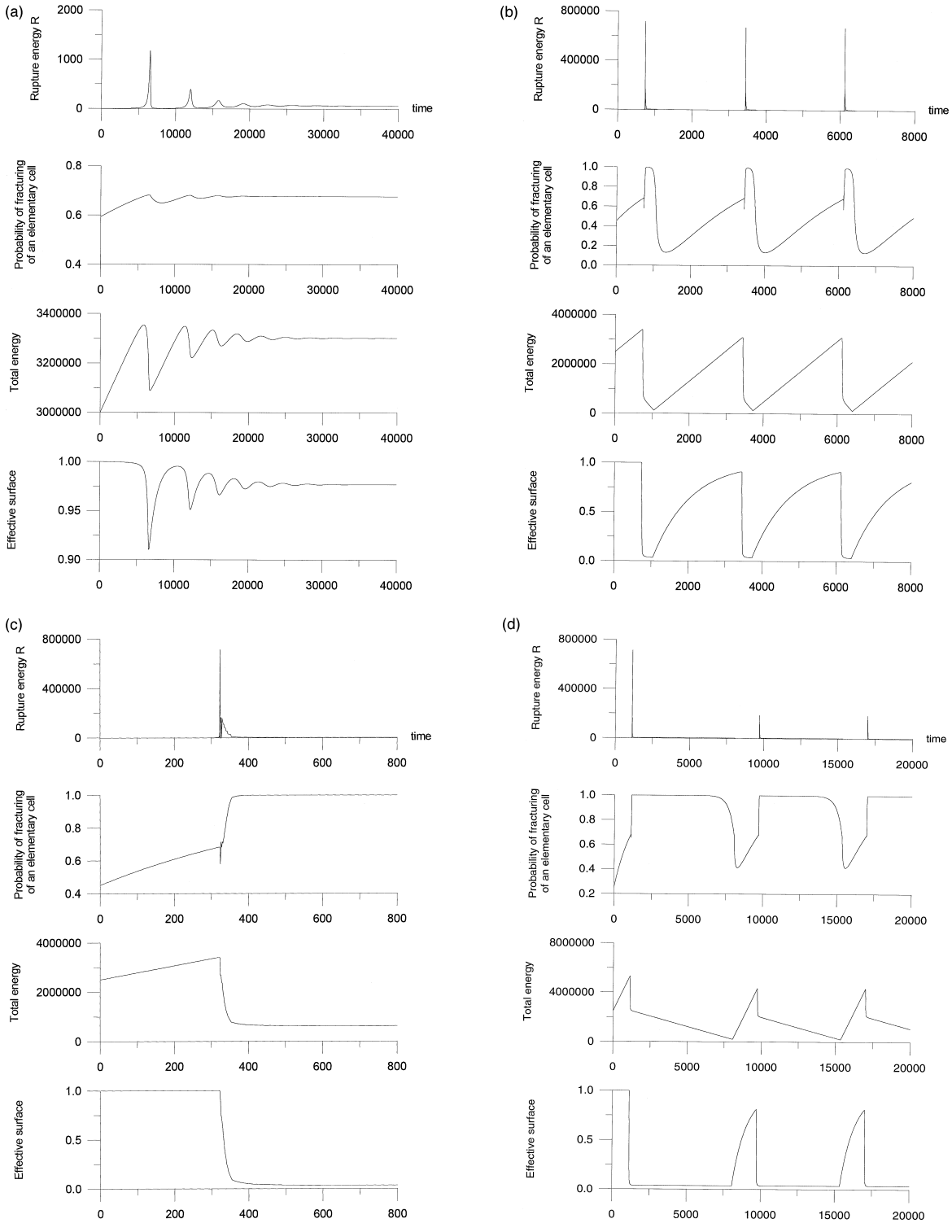
(a)
Rupture energy R
2000
1000
0
time
0
10000
20000
30000
40000
Probability of fracturing of an elementary cell
0.8
0.6
0.4
Total energy
3400000
3200000
3000000
Effective surface
1.00
0.95
0.90
(b)
Rupture energy R
800000
400000
0
time
0
2000
4000
6000
8000
Probability of fracturing of an elementary cell
1.0
0.8
0.6
0.4
0.2
0.0
Total energy
4000000
2000000
0
Effective surface
1.0
0.5
0.0
(c)
Rupture energy R
800000
400000
0
time
0
200
400
600
800
Probability of fracturing of an elementary cell
1.0
0.8
0.6
0.4
Total energy
4000000
2000000
0
Effective surface
1.0
0.5
0.0
(d)
Rupture energy R
800000
400000
0
time
0
5000
10000
15000
20000
Probability of fracturing of an elementary cell
1.0
0.8
0.6
0.4
0.2
Total energy
8000000
4000000
0
Effective surface
1.0
0.5
0.0

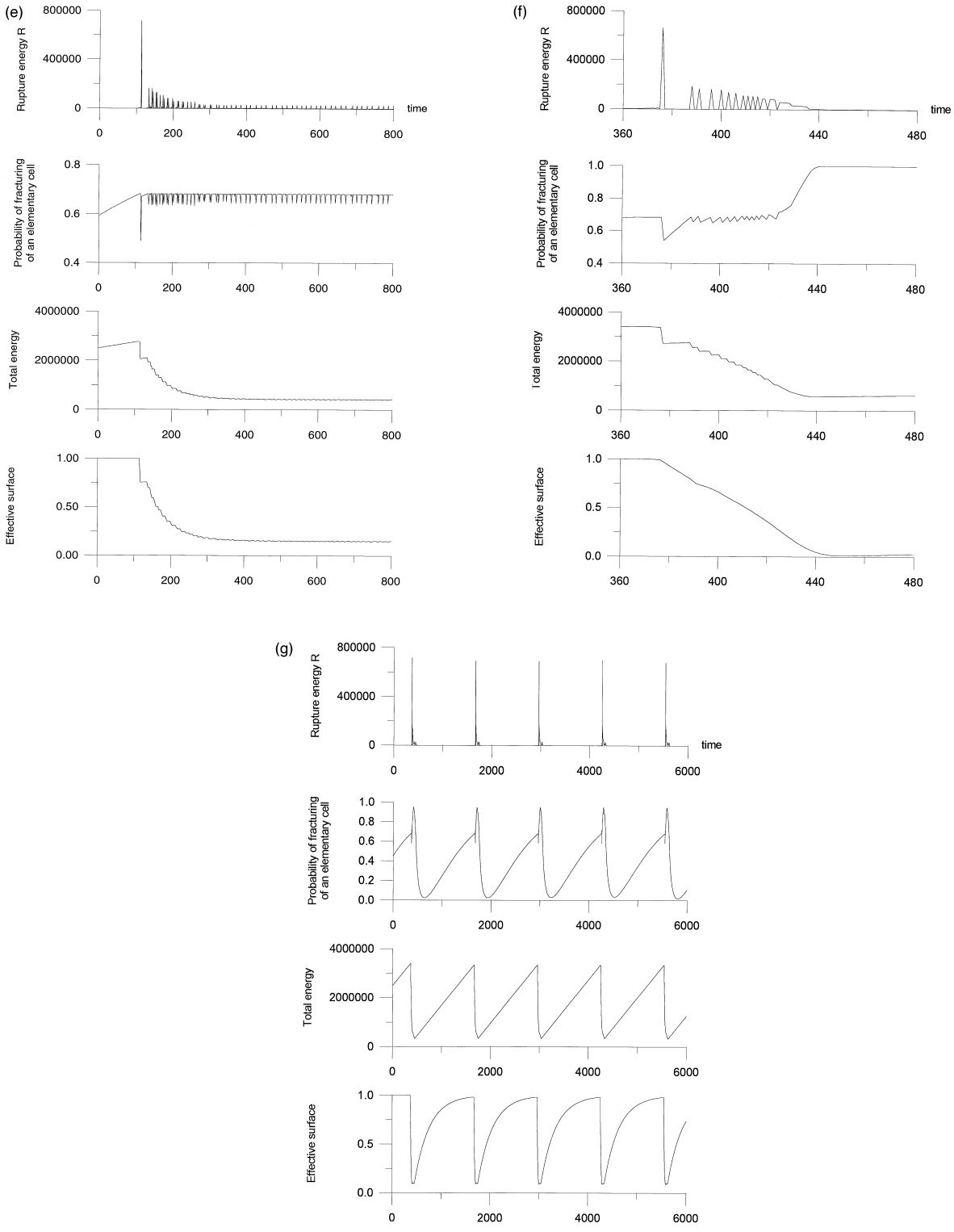
(e)
Rupture energy R
800000
400000
0
time
0
200
400
600
800
Probability of fracturing of an elementary cell
0.8
0.6
0.4
Total energy
4000000
2000000
Effective surface
1.00
0.50
0.00
(f)
360
440
480
1.0
0.5
0.0
(g)
2000
4000
6000
0.2

This allows us to use k directly for the earthquake magnitude.

Now we can theoretically construct the magnitude–frequency graphs corresponding to different values of the elementary probability $p_1(t)$ by taking the logarithm of Eq. (4) and using Eq. (13). Results are shown on Fig. 4. We consider one elementary time interval and take $S(t) = S_0$, $L = 15$, $\delta = 0.1$. If $p_1(t) \geq 0.6823$ (the critical value: $P(0.6823) = 0.6823$), the magnitude–frequency graph is practically linear with the slope $b = \log 9 = 0.95$. For lower values of p_1. Examples of magnitude–frequency graphs for longer time intervals will be given later in the numerical experiments.

2.3. Numerical experiments

As in the previous paper, we will examine both single domain and multiple domain cases. In the case of a single domain we will present one example which gives results similar to real seismicity data (Scholtz, 1990), then consider the influence on these results of varying the parameters of the model. Afterwards, considering two multidomain examples, we will examine the interaction of neighboring domains and demonstrate the possibility of earthquake triggering.

2.3.1. Single domain case

The modifications of the S.O.F.T. model described above allow us to obtain more realistic aftershock sequences and also to obtain a repetition of strong earthquakes (seismic cycle). This is demonstrated by a typical numerical experiment for the single domain case (Figs. 5–8) in which we used the following values of the parameters: $E_0 = 2.5 \times 10^6$; $\Delta E_0 = 2.5 \times 10^3$; $\alpha = 6.0 \times 10^{-7}$; $\varepsilon = 1.5 \times 10^6$; $\delta = 0.1$; $\lambda N = 0.1$; $\mu = 3.4 \times 10^{-7}$; $\sigma_1 = 3$; $\sigma_2 = 1000$; and $L = 15$. On Fig. 9 we present in addition the most interesting examples obtained by varying the parameters.

Repetition of strong earthquakes (Fig. 5) (Scholtz, 1982) is due to the balance between the energy coming from outside (integral of ΔE) and the energy dissipated through earthquakes (integral of R). In our typical experiment, the first and strongest (highest hierarchy level L) earthquake occurs at the end of the first loading interval. Afterwards the system is periodically reloaded and produces periodically strong events of level $(L-1)$; the surface S which can generate earthquakes does not reach again the value which is necessary for earthquakes of the maximum level of hierarchy (L) to occur.

The system is strongly self-organized, and its behavior remains the same in a wide diapason of parameters. For example, the balance of coming and dissipated energy remains if the value of ΔE_0 is decreased by a factor of two (Fig. 9b). In this new example the slow rate of coming energy allows the system to completely retrieve its initial state, and we observe a repetition of the strongest possible earthquakes.

In the typical experiment strong earthquakes are followed by sequences of *aftershocks* of all magnitudes (Fig. 6). The decrease in time of the number of aftershocks is self-similar (Fig. 8), as in the case of real aftershock sequences (Omori law: Utsu, 1965).

Foreshocks are less strong than aftershocks: in the typical experiment their maximum magnitude corresponds only to the third level of hierarchy from the top ($k = 13$) (Fig. 6). The slope of the magnitude–frequency graph corresponding to the foreshocks sequence is significantly higher than it is for reloading and aftershock phases (Fig. 7).

We have then, as announced supra, studied how varying the parameters affects the behavior of the model. The most interesting examples are shown on Fig. 9. A change of the initial energy E_0 can only shift the time scale (of course, if it does not immediately provide the critical value of p_1). As in the previous paper (S.O.F.T.1), the most important parameters are ΔE_0 and α (parameter α replaces parameter k in the previous paper).

Very small values of ΔE_0 give an a-seismic behaviour (Fig. 9a). But the level of total energy in this example is high enough (compare with Fig. 5a)

Fig. 9. Results of varying of the model parameters in comparison with the typical result. The values of parameters are the same as on Fig. 5 except: (a) $\Delta E_0 = 0.7 \times 10^2$; (b) $\Delta E_0 = 1.25 \times 10^3$; (c) $\Delta E_0 = 2.85 \times 10^3$; (d) $\alpha = 0.3 \times 10^{-6}$; (e) $\alpha = 0.9 \times 10^{-6}$; (f) $\sigma_1 = 15$; (g) $\sigma_2 = 300$.

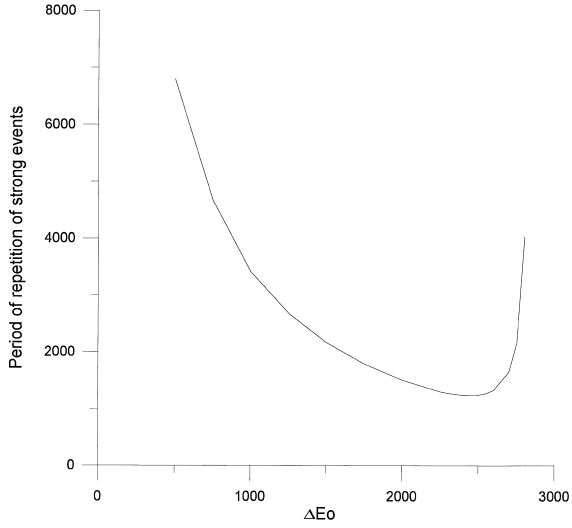

Fig. 10. The periodicity of strong earthquakes as a function of the parameter ΔE_0. All other parameters are as for Fig. 5. The limit for low values corresponds to the non-stable balance with high accumulated energy. The limit for high values corresponds to the stable balance with accumulated energy and permanent dissipation of energy by small events.

to produce the strongest earthquake and a small injection of additional energy can generate (trigger) this big event. We will show that later when considering multidomain examples. The opposite situation corresponds to high values of ΔE_0 (Fig. 9c): the strong earthquake largely destroys the domain; after this event only a very small part of the initial surface remains effective; this part generates permanently small events. Intermediate values of ΔE_0 provide a repetition of strong earthquakes as on Figs. 5 and 9b. Fig. 10 shows how the period of this repetition (the seismic cycle) depends on the value of ΔE_0 (all the other parameters being fixed).

Parameter α influences too the period of strong events repetition. Small values correspond to a slower energy dissipation rate and, accordingly, to larger values of this repetition period. Large values of α can produce a picture which seems to represent a discrete case (Fig. 9e: each event seems to be isolated from each other). In reality this is no more than the standard case but with a very short period of the seismic cycle. The decrease in time of the amplitude of R at the beginning is only a transitional period due to the chosen initial conditions.

Influence of parameter ε is similar but opposite to that of parameter α; small values of ε correspond to short periods of the seismic cycle. The parameter μ also provides longer seismic cycle periods when it is given larger values and produces the pseudo-discrete picture when it is given small values. The value of δ practically does not change the results if it varies in the range 0.05–0.5.

Parameter λ changes the energy scale, and has to be considered simultaneously with parameters ΔE_0, ε and α. The maximum hierarchy level L has be taken equal to 15 and no other value has been considered.

Larger values of the time delay σ_1, characteristic of the effective surface decrease after an event, can generate a seismic swarm as on Fig. 9f; the aftershocks sequence is replaced by a sequence of strong events of similar magnitude. σ_2 influences the length of the aftershocks sequence and the period of the seismic cycle. One example is shown on Fig. 9g.

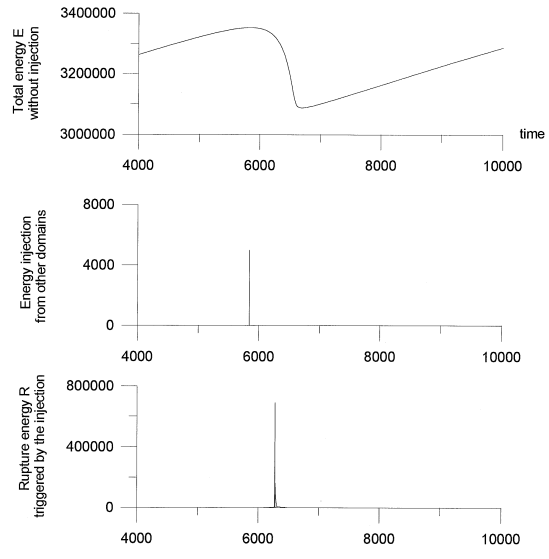

Fig. 11. Example of triggering a strong earthquake by a small energy injection. The graph at the top shows a fragment of the graph of R from Fig. 9a. Next graph shows the energy injection. The bottom graph represents values of R when the small energy injection has been added. The value of the injected energy is two orders of magnitude lower than the value of R generated by the top hierarchy level events.

2.3.2. Multidomain case

We present here two simple examples of interaction of several domains. The first example represents the possibility of triggering strong earthquakes. The second shows that even a small variability in time of the energy feeding the considered domain can significantly influence its seismicity (Keilis-Borok, 1994). We assume that this variability is produced by an interaction with a neighboring domain (part of the energy R dissipated in this second domain goes to the domain under consideration).

2.3.2.1. Earthquake triggering. We consider here the case of a very small rate of energy ΔE_0 (Fig. 9a) and inject into the domain an extra-amount of energy (Fig. 11); the value of this amount is 5×10^3, that is approximately $1/200$ of the energy of the strongest event. This injection acts as a triggering for generating an event of the highest level L. It is interesting to observe that this event occurs with some delay after the injection and is preceded by foreshocks. The energy of the event is two orders of magnitude higher than the value of the injected extra-amount of energy.

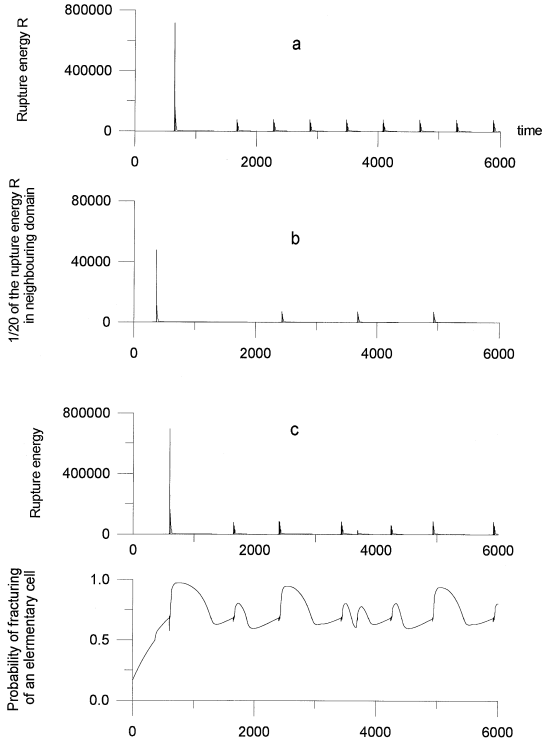

Fig. 12. Interaction of two domains. (a) rupture energy R for a domain with the same model parameters as for Fig. 5, except: $E_0 = 1.5 \times 10^6$ and $\varepsilon = 1.2 \times 10^6$; (b) rupture energy $(1/20)$ in the typical experiment (parameters as on Fig. 5); (c) resulting rupture energy and p_1 in the first domain.

2.3.2.2. Interaction of neighboring domains. Let us consider two domains (Fig. 12). In the first domain the parameters of the model are the same as in the typical experiment except for $E_0 = 1.5 \times 10^6$ and $\varepsilon = 1.2 \times 10^6$. The graph representing the rupture energy R for this case (without interaction) is shown on Fig. 12a. The second domain is exactly as in the typical experiment. We assume that $1/20$ of the rupture energy R of the second domain is transmitted to the first one. The average of this energy (Fig. 12b) per time unit is to 0.17×10^3. In order not to change the total energy which comes into the first domain, we subtract from ΔE_0 (corresponding to the first domain) this average value, but at every moment we add the instantaneous energy coming from the second domain. The result (graphs of R and p_1) is shown on Fig. 12c. The interval between strong events is no longer constant.

More complicated combinations of domains with different parameters will lead to more complicated results. We think that practically any sequence of events can be modeled in such a way.

3. Discussion and conclusions

In the present paper we have obtained a significant improvement of the previous S.O.F.T. model. First, we succeeded in obtaining the decrease in time of the number of aftershocks and of their energy, similarly to what is observed in the case of the real earthquakes (Omori law). Secondly, due to the introduction of energy redistribution by creep, we have obtained the repetition of the seismic cycle, with periods of low level of seismic activity, periods of activation (foreshocks), followed by a strong main shock and aftershocks.

We model creep by an apparent reconstruction of the surface of the domain at a rate proportional to the size of the broken area (Eq. (7)). This can be ex-

plained as well in terms of heterogeneity of the energy distribution in the domain. We model this heterogeneity by two homogenous parts of the domain: a broken part, in which the potential energy is zero, and a non broken part, in which the density of potential energy is constant. This is a kind of description of asperity or barrier type (Aki, 1984). In such words, the redistribution of energy is equivalent to an increase of the size of the unbroken part.

The apparent surface reconstruction we spoke above has nothing to do with the process of consolidation of the broken material. We guess that consolidation process is incomparatively slower.

3.1. How does the model work?

Periods of low seismic activity (seismic noise) correspond to the relatively long periods of loading (or reloading) of the system, when the energy comes from outside much faster than it is dissipated by small events. During these periods the density of energy is below the critical value.

As the energy density approaches the critical value, the seismic activity increases. In our model foreshocks start earlier at lower levels of scaling (lower magnitude of events); they may be absent at higher levels. During the foreshock period the energy continues to accumulate, because the foreshocks energy is weak.

Finally, a significant part of the accumulated energy is released in the strong earthquake which breaks part of the domain. The remaining potential energy is passed to the unbroken part (possibly with some small delay). At the beginning the relative losses in area of the sound domain are higher than the relative losses of energy. This gives a further increase of the energy density, and aftershocks start. The number per unit time and energy of the quakes are now limited by the size of the unbroken part of the domain. The energy released by aftershocks is enough for the total density energy of the system continue to drop down. The 'working' surface at some point stabilizes—when losses of the sound surface become equal to the apparent recovering of surface by creep. Those two processes together lead to a decreasing of the energy density. At some moment this density drops below the critical value, and the aftershock sequence transforms into seismic noise (we have to note that in the present model the beginning of the aftershock sequence is accompanied by an increase of the energy concentration).

Thus, the frame of this model, characterized by a reasonably small number of parameters, has provided in numerical experiments a behavior presenting some gross properties of real seismicity: Gutenberg–Richter law, Omori law, seismic cycle.

Let us emphasize again a main characteristic of the model—tectonic energy enters it at the smallest scale and cascades up to larger scale levels. This is compatible with the asperities mechanism as defined by Aki (1984)—asperities represent smaller scale heterogeneities than the whole fault plane, and the process creating asperities involves foreshocks and precursing creep; the fault plane becomes heterogeneous before the rupture and the main shock is a stress smoothing process over the fault plane. But, as pointed out by one of the referees, the barrier mechanism rather calls for a cascading down of energy. Barriers, as defined by the same paper of Aki (1984), represent small scale heterogeneities created by the main shock rupture. Non-uniform slip over the fault plane creates stress concentration over it, causing aftershocks along the mainshock rupture plane. The main rupture is in this case a stress roughening process, and smaller events are created by larger events. Tectonic energy enters the system from the largest scale, through plate motion, and is cascaded down to smaller scales.

Both cascading up and down may be simultaneously working in the actual fault zone, but, according to the referee, observations support the evidence of cascading down. For example, he says, foreshocks are subtle and rare phenomena, while aftershocks are ubiquitous and robust. But this one observation does not, in our opinion, contradict the inferences of the present model: foreshocks are often present only at the smallest scales and then have very small energy, whereas aftershocks are ubiquitous and much more energetic (Section 2.3.1) even without introducing cascading down. Nevertheless cascading down is certainly to be introduced into the model, without giving up its main ingredient, i.e. large scale self-organization from small scale events. This will be one of our next steps. Together with the introducing of other physical concepts, like nucleation and growth, and heterogeneities, it will allow us, we

hope, to closer approach the rupture dynamics and to account for more observations on earthquakes than the Gutemberg–Richter and Omori law.

Acknowledgements

We thank the referees for judicious comments. The present work was completed in IPG Paris while P. Shebalin had a visitory scientist grant within the IPG-MITPAN cooperation agreement. The present work was also supported by the Russian Foundation of Fundamental Research (Project Code 93-05-8870) and by INTAS Foundation (Project Code INTAS-93-457). IPGP contribution.

References

Aki, K., 1984. Asperities, barriers, characteristic earthquakes and strong motion prediction. J. Geophys. Res. 86, 5867–5872.

Allègre, C.J., Le Mouël, J.L., 1994. Introduction of scaling techniques in brittle fracture of rocks. Phys. Earth Planet. Inter. 87, 85–93.

Allègre, C.J., Le Mouël, J.L., Provost, A., 1982. Scaling rules in rock fracture and possible implications for earthquake prediction. Nature 297, 47–49.

Allègre, C.J., Le Mouël, J.L., Ha Duyen, C., Narteau, C., 1995. Scaling Organisation of Fracture Tectonics (S.O.F.T.) and earthquakes mechanism. Phys. Earth Planet. Inter. 92, 215–233.

Blanter, E.M., Shnirman, M.G., 1996. Self-organized criticality in hierarchical model of defects development. Phys. Rev. E. 53, 3408.

Blanter, E.M., Shnirman, M.G., Le Mouël, J.L., Allègre, C.J., 1997. Scaling laws in blocks dynamics and dynamic self organized critically. Phys. Earth Planet. Inter. 99, 295–307.

Gutenberg, B., Richter, C.F., 1954. Seismicity of the Earth and Associated Phenomena, 2nd edn., Princeton Univ. Press, 310 pp.

Hattori, S., 1974. Regional distribution of *b* value in the world. Bull. Int. Seismol. Earth Eng. 12, 39–58.

Ito, K., Matsuzaki, 1990. Earthquakes as self-organised critical phenomenon. J. Geophys. Res. 95, 6853–6860.

Kanamori, K., Anderson, D.L., 1975. Theoretical basis of some empirical relations in seismology. Bull. Seismol. Soc. Am. 65, 1073–1096.

Keilis-Borok, V.I., 1990. The lithosphere of the Earth as a nonlinear system with implications for earthquake prediction. Rev. Geophys. 28 (N1), 9–34.

Keilis-Borok, V.I., 1994. Sympthoms of instability in a system of earthquake-prone faults. Physica D 77, 193–199.

King, G.C.P., 1978. Geological faults: fracture, creep and strain. Phil. Trans. R. Soc. Lond. A.288, 197–212.

King, G.C.P., 1983. The accomodation of large strains in the upper lithosphere of the Earth and other solids by self-similar fault system : the geometrical origin of the b-value. PA-GEOPH 121, 567–585.

Kranz, R.L., 1979. Crack growth and development during creep of Barre granite. Int. J. Rock Mech. Min. Sci. 16, 23–35.

Narkunskaya, G.S., Shnirman, M.G., 1990. Hierarchical model of defects development and seismicity. Phys. Earth Planet. Inter. 61, 29–35, 200-216.

Okal, E.A., Romanowicz, B.A., 1994. On the variation of b-values with earthquake size. Phys. Earth Planet. Inter. 87, 55–76.

Scholtz, C.H., 1982. Scaling laws for large earthquakes: consequences on physical models. Bull. Seismol. Soc. Am. 72, 1–14.

Scholtz, C.H., 1990. The Mechanics of Earthquakes and Faulting, Cambridge Univ. Press, UK.

Turcotte, D.L., 1992, Fractals and Chaos in Geology and Geophysics, Cambridge Univ. Press, UK.

Utsu, T., 1961. Statistical study on the occurence of aftershocks. Geophys. Mag. 30, 521–605.

Utsu, T., 1965. Aftershocks and earthquake statistics. J. Fac. Sci. Hokkaido Univ. Ser. VII 3, 379–441.

Wilson, K.G., 1979. Problems in physics with many scales of length, Sci. Am., August, pp. 140–157.